KFUPM
Journal of Undergraduate Research International

Diamond Open Access 1

Article Aerospace Engineering

Deployable Solar Panels as Passive Drag Surfaces for Satellite Deorbiting

Teef Alharthi and Asia Habila*

Cite https://doi.org/10.64589/juri/231567

Submitted: November 29, 2025 Revised: May 02, 2026 Accepted: May 15, 2026

ABSTRACT

Space debris, including non-operational satellites, is a growing issue affecting the safety of the space environment. This study evaluates the potential application of solar panels as deployable structures for passive deorbiting, building on previous studies that have demonstrated the influence of satellite surface area on atmospheric drag. These deployable structures can generate power during satellite operations and increase the aerodynamic drag post-mission to aid deorbiting. A 6U CubeSat (8 kg) operating in a 525-km sun-synchronous orbit was modeled using the high-precision orbit propagator within the systems tool kit (STK) along with the NRLMSISE2000 atmospheric density model. Three solar panel deployment configurations were analyzed and compared with a fixed-panel baseline to examine the trade-off between orbital lifetime and power generation. The results showed that changing the panel deployment angle alone reduced the orbital lifetime from 21.0 to 11.6 years, as the increased cross-sectional area enhanced atmospheric drag. However, the configurations that produce the maximum drag also reduce the amount of sunlight that the solar panels receive thereby reducing the power generated. Furthermore, increasing the solar exposure area while keeping the drag area constant has a negligible effect on the orbital lifetime at this altitude. The results demonstrate that solar panels can act as passive drag devices to enable significant lifetime reduction while maintaining operational capabilities. This method can assist in meeting the requirements of space debris mitigation guidelines, which require limiting post-mission lifetimes.

Keywords: passive deorbiting, deployable solar panel, atmospheric drag, CubeSat, satellite lifetime reduction, space debris mitigation

1. INTRODUCTION

With the rapid growth of the space industry, the amount of space debris, including non-operational satellites, discarded rocket stages, fragments, and collisional debris, has increased significantly. Recently, the number of debris objects with diameters of 1–10 cm orbiting in geostationary, equatorial, and low Earth orbit (LEO) regions has exceeded 1 million [1]. The large amount of space debris and its high speed can harm satellites and missions. This growing concern emphasizes the need to implement effective mitigation measures. Non-operational satellites represent a major source of space debris. Currently, approximately 2800 inactive satellites orbit Earth [2]. An effective solution to mitigate this issue is deorbiting, a process in which non-functioning satellites are removed from orbit by re-entering them into the atmosphere, where they burn upon re-entry. There are two main deorbit methods: passive and active deorbiting. Active deorbiting uses external mechanisms, such as thrusters, robotic arms, or dedicated space missions, to force lower satellites to re-enter the atmosphere. This method has the drawbacks of high costs associated with deorbiting maneuvers and fuel consumption. Consequently, passive deorbiting methods use natural forces such as atmospheric drag, solar radiation pressure, and interaction with Earth's magnetic field. These techniques are particularly advantageous for small satellites such as 6U CubeSats. Therefore, passive deorbiting methods are optimal solutions for the given application. Passive methods include drag sails, which use deployable surfaces that increase a satellite's cross-sectional area; solar sails, which use reflective surfaces that exploit solar radiation pressure; electrodynamic tethers, which use long conductive wires to interact with Earth's magnetic field; and inflatable structures, which employ expandable components to increase atmospheric drag.

According to the national aeronautics and space administration (NASA) [1], atmospheric drag as an effect only when the debris altitude is less than 250 km, leading to exponentially long space debris orbital lifetimes. The speed at which a spacecraft deorbits in LEO is determined by multiple elements, including its initial deployment altitude, aerodynamic properties such as the ballistic coefficient, and space weather activity. These factors are essential for ensuring adherence to end-of-life disposal guidelines [1]. Major efforts have been made regarding end-of-life disposal regulations. For example, on September 29, 2022, the U.S. federal communications commission (FCC) introduced a new regulation requiring that all FCC-licensed satellites operating in LEO must be deorbited or disposed of within five years after the end of their mission [1]. Similar requirements have been

Published under an exclusive license by KFUPM

adopted by the European space agency (ESA)[3].This regulatory shift underscores the urgency of developing reliable, low-cost passive deorbiting solutions that can be integrated into the satellite design, particularly for small satellites lacking onboard propulsion[1,3]. Previous studies have investigated how to reduce the amount of existing space debris using both active and passive methods. Ru et al.[4] proposed a method for actively removing debris using a flexible net system, which they tested using numerical simulations. Their results demonstrated that the net successfully captured rotating debris at an angular velocity of 6.28 rad/s and dragged it along a controlled trajectory. Chen et al.[5] analyzed the effect of drag sails on CubeSat aerodynamic performance as a passive deorbiting method using the direct simulation Monte Carlo (DSMC) method. The DSMC method is a particle-based statistical method for simulating rarefied gas flows, in which the molecular mean free path becomes comparable to body size characteristics (i.e., at high Knudsen numbers) and continuum computational fluid dynamics (CFD) assumptions break down, making it particularly appropriate for the low-density LEO environment considered here[6]. Their results indicated that a drag sail substantially enhanced the drag force on the CubeSat, confirming that an increased cross-sectional area led to shorter deorbiting times, which is consistent with the area-to-mass ratio principle employed in this study[5]. Chandra and Thangavelautham[7] evaluated two inflatable drag concepts for CubeSats using structural simulations and showed that both designs significantly reduced the orbital lifetime. Jiang et al.[8] created a dynamic model that combined brake sails and electrodynamic tethers. They used numerical simulations to show that the hybrid design was better at deorbiting satellites than single methods. A previous study[9] demonstrated the effectiveness of using aerodynamic drag by developing an analytical-numerical targeting algorithm that adjusted the spacecraft's drag profile to control the reentry location, achieving an average targeting error below 200 km using only aerodynamic drag. The DeOrbitSail project[10], funded by the EU FP7 program and coordinated by the University of Surrey, aims to demonstrate deorbiting using a deployable sail on a 3U CubeSat platform. The satellite uses four deployable booms to unfold a 4×4m sail membrane, achieving a frontal area of 16 $m^2$and weighing less than 6 kg. The increased cross-sectional area enhanced the aerodynamic drag, and the project demonstrated that the sail could deorbit the satellite from 650 km within 120 days.

Although deorbiting methods have been widely studied, the use of deployable solar panels as dual-function structures for power generation and passive drag enhancement has received little attention in the context of post-mission deorbiting. Barato[11] analyzed the optimal use of deployable solar panels in a very LEO and showed that even relatively small panel inclinations with respect to the velocity vector significantly increase drag, highlighting the inherent trade-off between panel orientation for power generation and drag minimization. However, that study focused on drag compensation during active operations using electric propulsion rather than leveraging panel drag for end-of-life disposal. Mungiguerra et al.[12] analyzed the aerodynamic behavior of a satellite equipped with deployable aerobrakes and solar panels and confirmed that solar panels contribute to increased drag and improved longitudinal stability.

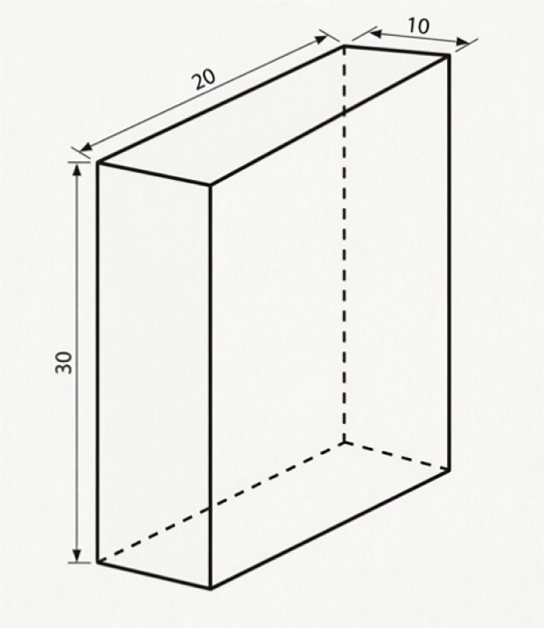


Figure 1. proposed satellite configuration

However, they did not focus on analyzing drag for deorbiting. By contrast, the present study focused specifically on evaluating how different solar panel deployment angles affect the drag area, and consequently, the orbital lifetime of a 6U CubeSat. Unlike Mungiguerra et al.[12], who primarily examined aerodynamic stability, this study quantified the trade-off between drag-induced lifetime reduction and power generation across multiple configurations, directly addressing the need for compliance with current space debris mitigation regulations[1,3].

2. METHODOLOGY

2.1. Mission Scenario and Assumptions. In this section, the methodology used to evaluate the effectiveness of different solar panel configurations on atmospheric drag is described in detail. Two scenarios were considered in the evaluation. The first scenario was a fixed-body solar panel configuration without deployment. The second scenario considered different solar panel deployment angles to allow for a fair comparison and clear evaluation.

In both scenarios, the proposed satellite was a 6U CubeSat with a total mass of 8 kg and dimensions of 10 cm ×20 cm ×30 cm, as shown in Figure 1. The CubeSat should be in a sun-synchronous orbit (SSO) 525 km above Earth, with an inclination of approximately 98°. The satellite was assumed to operate without propulsion and was affected by atmospheric drag and solar activity. Furthermore, the satellite was assumed to maintain a fixed attitude throughout the decay, with the solar panels oriented to maximize power generation for each configuration. Although this is an idealization, it ensures that the drag area presented to the flow remains constant and predictable for each configuration. In practice, tumbling or attitude uncertainty changes the time-averaged drag area, potentially changing both the power

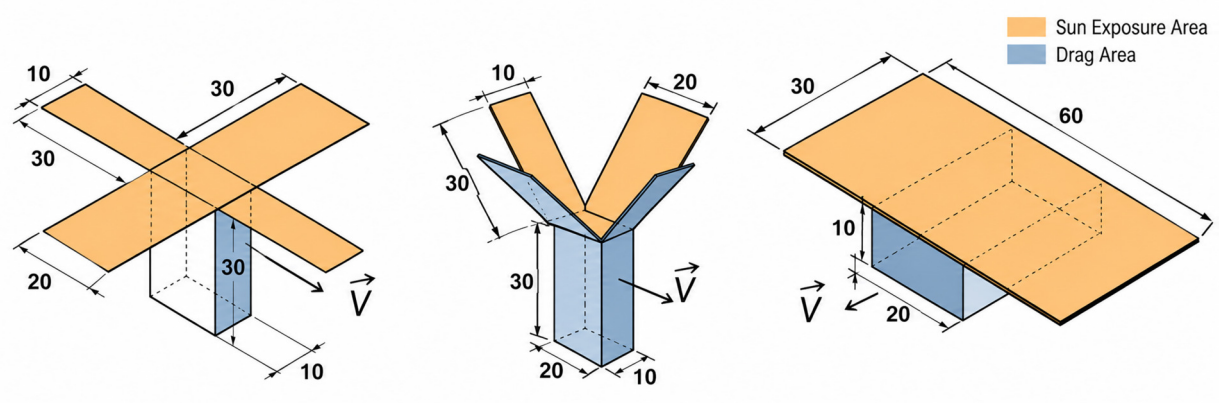


Figure 2. Proposed configurations with the velocity vector direction. 2.A. Configuration (A): four flat solar panels deployed perpendicular to the satellite body, giving a drag area of 0.03 m^2. 2.B. Configuration (B): four solar panels deployed at a 45°angle to the satellite body, increasing the drag area to 0.0512 m^2. 2.C. Configuration (C): two large solar panels double-deployed along the long edge (long axis) of the CubeSat, giving a minimal drag area of 0.02 $m^2$with maximized solar exposure

output and deorbiting rate [11,13]. Future studies should incorporate stochastic variations in the ballistic coefficient to account for attitude dynamics effects.

2.2. Passive Deorbiting Concept. In LEO, atmospheric particles exert drag on orbiting satellites, causing gradual orbital decay. The drag force can be described follows [14]:

$$F_d = C_D A \frac{\rho V^2}{2} \quad (1)$$

where F_d is the drag force, C_D is the drag coefficient, ρ is the atmospheric density, A is the cross-sectional area of the satellite perpendicular to the flow, and V is the satellite's orbital velocity [14].

The maximum power generated by the solar panels is given by:

$$P = A_{panel} \times 1361 \times \eta \times \cos(\theta) \quad (2)$$

where A_{panel} denotes the effective solar panel area. The value of 1361 W/m^2 is the solar constant, which represents the amount of solar energy arriving at 1 m^2 at the top of Earth's atmosphere when the panel directly faces the Sun; it is based on precise satellite measurements, such as NASA's SORCE/TIM instrument. η denotes the solar panel efficiency [15].

A key parameter that affects the decay rate is the area-to-mass ratio (AMR). Satellites with a larger cross-sectional area relative to their mass experience higher drag, leading to faster deorbiting. Deployable solar panels have been used to increase the AMR to passively deorbit satellites.

2.3. Simulation Setup. For lifetime analysis, this study employed the AGI Systems Tool Kit (STK), a mission simulation software used for modeling spacecraft trajectories, environmental perturbations, attitude dynamics, and lifetime prediction. In the simulations, the High-Precision Orbit Propagator (HPOP) within the STK Astrogator module was used. Although STK provides simpler propagators, such as the Two-Body and J2 models, HPOP was selected because it accounts for non-spherical Earth gravity, solar and geomagnetic activity, and atmospheric density variation factors. Additionally, atmospheric drag was modeled using the NRLMSISE 2000 density model, which is considered an accurate model for LEO because it provides the temperature, composition, and neutral density from the ground level to the exosphere and is driven by solar flux (F10.7) and geomagnetic activity (Ap) [14]. Compared to older models, such as Jacchia 1970 or Harris–Priester, NRLMSISE-2000 captures short-term space-weather variations more reliably, making it better suited for long-term orbital decay prediction. The HPOP was configured with a 60-s integration step size. The Earth gravity model used was EGM2008, with a degree and order of 21 ×21, and third-body perturbations from the Sun and Moon were included. The drag model employed a drag coefficient of $C_D = 2.2$, a satellite mass of 8 kg, and the drag area was varied according to each configuration, as described in detail in Section 2.4 (Table 1). Solar activity was modeled using a Space Weather file (SolFlx_CSSI.dat) from CelesTrak. The orbital parameters were set as follows: a circular orbit at 525 km altitude, inclination of 98°, and eccentricity near zero.

2.4. Solar Panel Configurations. The configurations to be tested, as shown in Figure 2, are based on Ibrahim and Yamaguchi [15]. The baseline configuration (A) comprised four, flat deployable solar panels attached perpendicularly to the satellite body. The second configuration (B) comprised four panels, deployed at a 45 ° angle to the satellite body. Configuration

Table 1. *Drag and solar exposure areas*

Configuration	Total Drag Area (A_D)	Solar Exposure Area
A	0.1×0.3 = 0.03 m^2	0.02+2(0.3×0.2) +2(0.3×0.1) = 0.2 m^2
B	0.3sin(45) ×0.1+0.1×0.3 = 0.0512 m^2	0.02+2(0.3sin(45) ×0.1)+ 2(0.3sin(45) ×0.2) = 0.1473 m^2
C	0.2×0.1 = 0.02 m^2	0.3×0.6 = 0.18 m^2

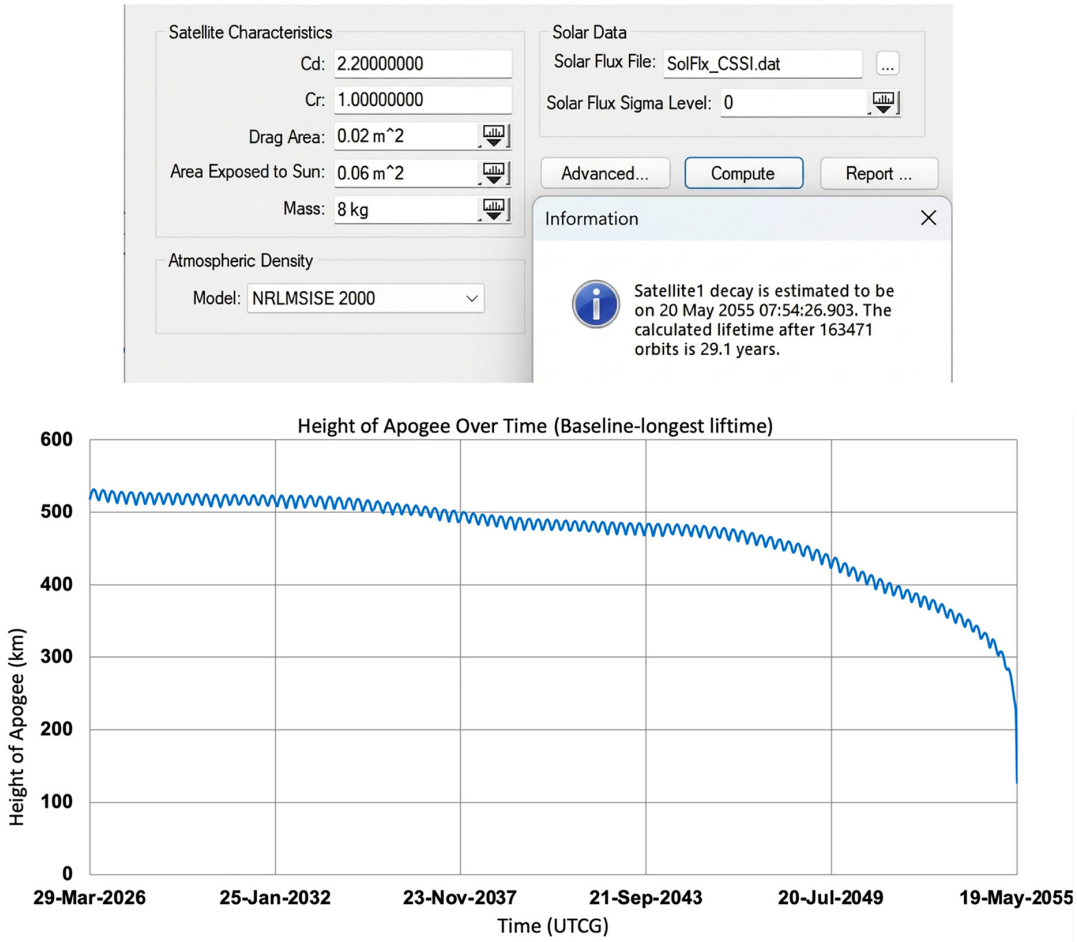


Figure 3. Simulated lifetime and drag and solar exposure areas for the baseline scenario

comprised double-deployed long-edge panels that is, two large deployable solar panels extending along the long axis of the CubeSat. The drag and solar exposure area calculations are presented in Table 1. For each configuration, the satellite was oriented such that the solar panels faced the Sun as much as possible, while having the smallest cross-sectional area relative to the velocity vector. This ensures that each configuration is evaluated for its best-case scenario in terms of power generation and longest orbital lifetime.

2.5. Evaluation Metrics. The performance of each solar panel configuration was evaluated using the lifetime, altitude decay rate, and trade-off between drag and power. Orbital lifetime is the time required for the satellite to decay from its initial 525-km orbit to atmospheric re-entry at an altitude of 122 km [16]. Additionally, the altitude decay rate was measured to understand how quickly each configuration reduced the semi major axis over time under varying drag forces. The results of this study were validated by comparison with previous analytical models and the literature.

3. RESULTS AND DISCUSSION

This section presents the outcomes of the two scenarios considered for evaluation: the baseline scenario with body-fixed solar panels and the other scenario with deployable solar panel configuration in terms of orbital decay.

3.1. Baseline Scenario. For the baseline case shown in Figure 2, the satellite operates with fixed solar panels and a minimal drag area of 0.02 m^2 and exposed solar area of 0.06 m^2 (Figure 3). The STK simulation results show a very slow orbital decay, resulting in a long lifetime of 29.1 years, which reflects limited aerodynamic interaction at 525 km. Throughout the mission, apogee and perigee remained stable (Figure 3).

3.2. Deployable Solar Panel Configurations. The lifetime analysis results for the deployable configurations are presented below.

In Configuration A, as shown in Figure 4, the drag area increases to 0.03 m^2, leading to a faster decay rate. STK predicted a lifetime of 21.0 years. For Configuration B, as shown in Figure 5, the drag area reaches 0.0512 m^2, resulting in a lifetime of 11.6 years. Configuration C, with a drag area of 0.02 m^2, yields a lifetime of 29.0 years, as shown in Figure 6. The generated power for each configuration is presented in Table 2.

The results indicate that the solar panel configuration plays a crucial role in orbital decay. Specifically, when comparing Configurations A and B, the lifetime decreased from 21.0 to 11.6 years just by changing the solar panel angle, as it increased the cross-sectional area and atmospheric drag and accelerated deorbiting. However, increasing the drag area by deflecting the panels results in reduced power generation as the panels are no longer perpendicular to the Sun. It is also noted by comparing Configuration

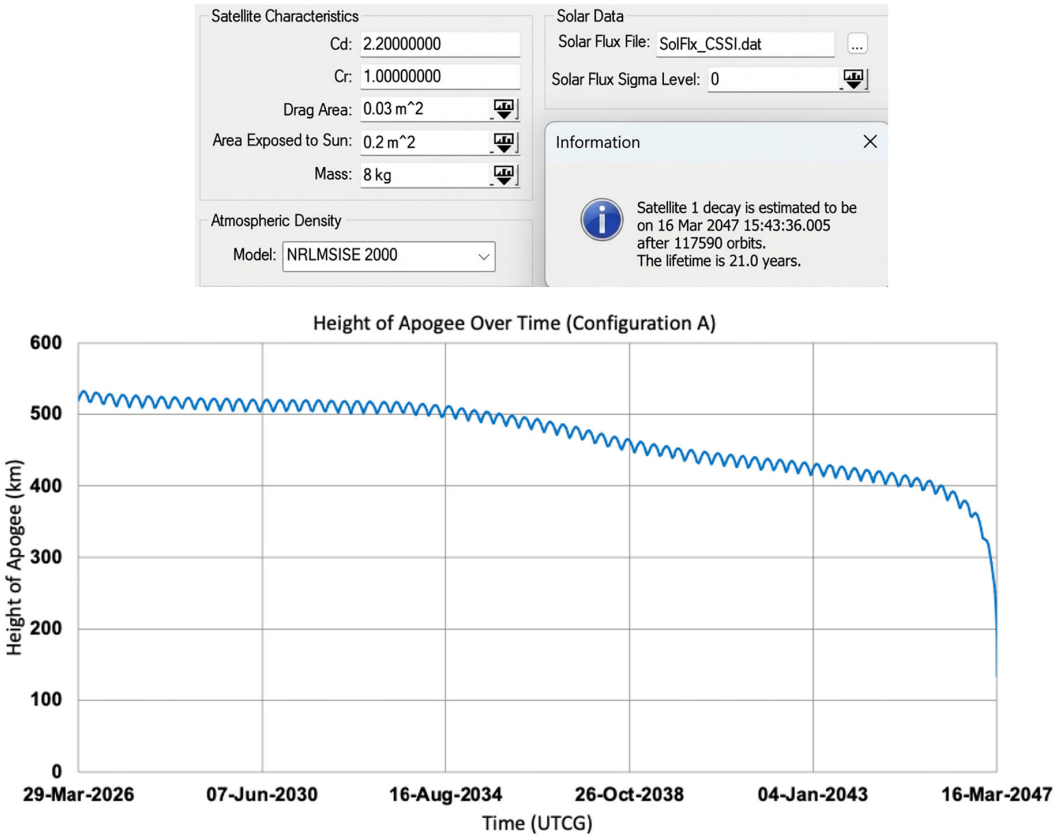


Figure 4. Simulated lifetime and drag and solar exposure areas for Configuration A

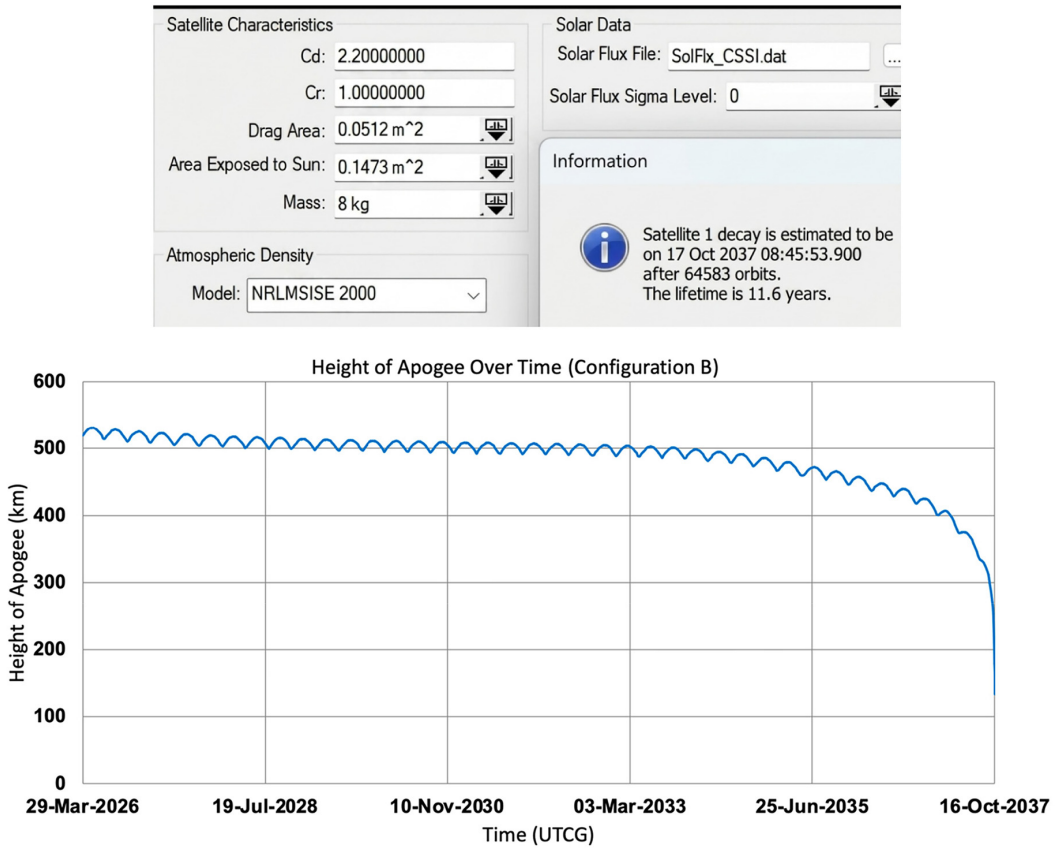


Figure 5. Simulated lifetime and drag and solar exposure areas for Configuration B

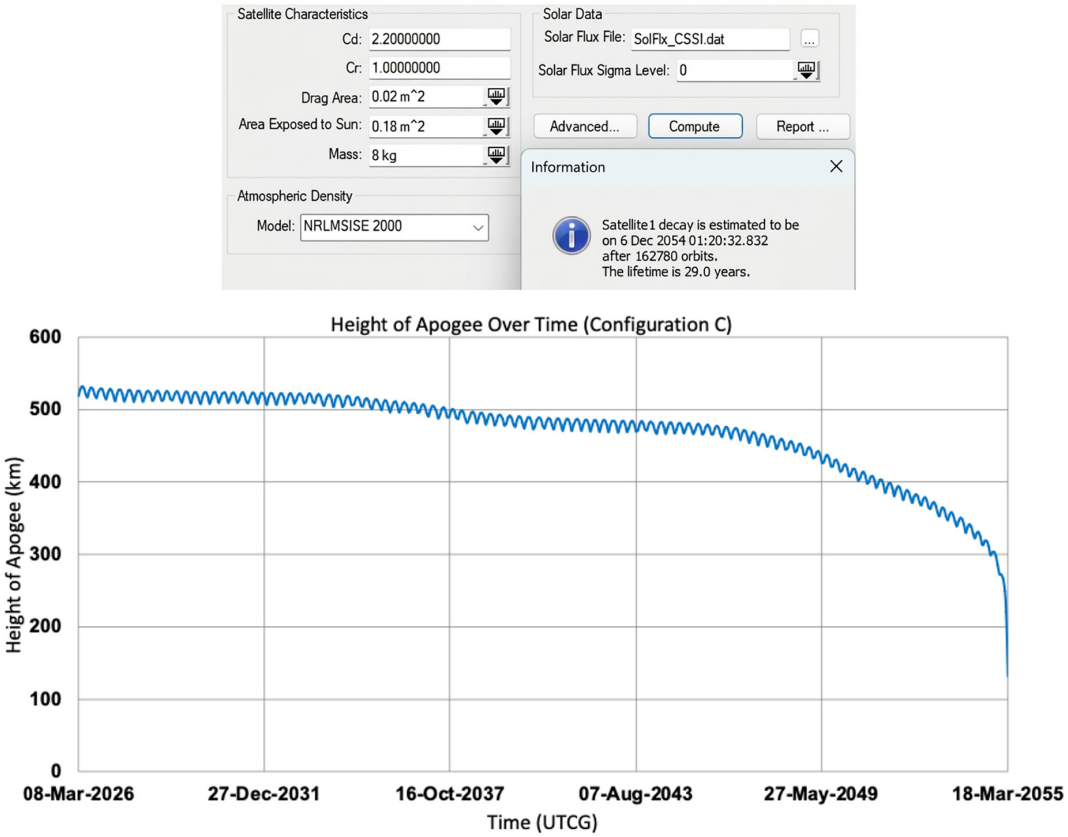


Figure 6. Simulated lifetime and drag and solar exposure areas for Configuration C

Table 2. *Trade-off comparison*

Configuration	Lifetime (years)	Generated Power (W)	Altitude decay rate (km/day)
A	21.0	49	0.33
B	11.6	24.5	0.34
C	29.0	32.7	0.32

C with the baseline, that increasing the solar exposure area while maintaining the drag area has a minor effect on the satellite's lifetime at this altitude.

For all configurations, the initial perigee altitude was approximately 512.30 km. After one day, the perigee for Configurations A, B, and C decreased to 511.97, 511.96, and 511.98 km, respectively. These values correspond to altitude decay rates of 0.33, 0.34, and 0.32 km/day, respectively. These results are based on a single simulation with specific solar activity inputs. The atmospheric density at LEO altitudes varies significantly with the solar cycle, geomagnetic storms, and seasonal effects [14]. During periods of high solar activity, the atmospheric density at 525 km can increase by one order of magnitude, substantially accelerating orbital decay. Future studies should incorporate Monte Carlo analyses across different solar cycle phases to determine the sensitivity of orbital lifetime predictions to space weather changes.

4. CONCLUSIONS

The growing issue of space debris is making the space environment increasingly dangerous and affecting existing satellites by increasing the drag area. Simulation results demonstrate the effectiveness of this approach, as the most favorable configuration reduced the orbital lifetime by more than half relative to the baseline case. In this study, the baseline showed a lifetime of 29.1 years, whereas the deployed configurations showed lifetimes of 21.0, 11.6, and 29.0 years, demonstrating the ability of solar panels to serve the dual functions of power generation and passive drag enhancement. Despite its many advantages, this study suffers from certain limitations, for example, the ideal orientation and stable deployment assumptions. In reality, attitude uncertainty can alter both the effective drag and power-generating areas; a tumbling satellite may present a time-averaged cross section that is significantly different from the assumed fixed orientation. Additionally, our findings are based on a single set of solar activity conditions, and sensitivity analyses across different solar cycle phases are recommended for future work.

AFFILIATIONS AND AUTHOR DETAILS

Undergraduate Author

Teef Alharthi – *Department of Aerospace Engineering, King Fahd University of Petroleum & Minerals, Dhahran 31261,*

Saudi Arabia; 0009-0002-7792-5979
Email: s202272900@kfupm.edu.sa

Corresponding Author

Asia Habila – *Research Mentor, Postdoctoral Researcher, Interdisciplinary Research Center for Aviation and Space Exploration, King Fahd University of Petroleum & Minerals, Dhahran 31261, Saudi Arabia*; 0000-0002-6155-2832
Email: asia.habila@kfupm.edu.sa

ACKNOWLEDGEMENTS

The authors acknowledge the support provided by the Department of Interdisciplinary Research Center and the Department of Aerospace Engineering at King Fahd University of Petroleum and Minerals.

REFERENCES

(1) State-of-the-Art of Small Spacecraft Technology. https://www.nasa.gov/smallsat-institute/sst-soa/deorbit-systems/ (2025).

(2) Space debris by the numbers. ESA's Space Debris Office. https://www.esa.int/Space_Safety/Space_Debris/Space_debris_by_the_numbers (2025).

(3) ESA Space Debris Mitigation Requirements (ESSB-ST-U-007, Issue 1). ESA (Oct. 2023). https://technology.esa.int/upload/media/ESA-Space-Debris-Mitigation-Requirements-ESSB-ST-U-007-Issue1.pdf

(4) Ru, M., Zhan, Y., Cheng, B. & Zhang, Y. Capture dynamics and control of a flexible net for space debris removal. *Aerospace* **9**, (2022). doi:10.3390/aerospace9060299.

(5) Chen, J., Chen, S., Qin, Y., Zhu, Z. & Zhang, J. Aerodynamic analysis of deorbit drag sail for CubeSat using DSMC method. *Aerospace* **11**, (2024). doi:10.3390/aerospace11040315.

(6) Tumuklu, A., Li, Z., Gimelshein, S. F. & Levin, D. A. Comprehensive evaluation of the massively parallel direct simulation Monte Carlo kernel 'Stochastic Parallel Rarefied-Gas Time-Accurate Analyzer' in rarefied hypersonic flows—Part A: fundamentals. *Computation* **12**, 198 (2024). doi:10.3390/computation12100198.

(7) Chandra, A. & Thangavelautham, J. De-orbiting small satellites using inflatables. (2018). doi:10.48550/arXiv.1809.04459.

(8) Jiang, H., Zhong, R. & Qi, R. Electrodynamic tether and brake sails combination deorbit design. *Acta Astronaut.* **226**, 669–678 (2025). doi:10.1016/j.actaastro.2024.11.007.

(9) Omar, S. R. et al. Spacecraft deorbit point targeting using aerodynamic drag. *J. Guid. Control Dyn.* **40**, 2646–2652 (2017). doi:10.2514/1.G002612.

(10) De-Orbiting of Satellites using Solar Sails. https://cordis.europa.eu/project/id/263248/reporting (2015).

(11) Barato, F. Optimal use of electric propulsion for drag compensation in very low earth orbit on satellites with deployable solar panels. *Acta Astronaut.* **213**, 1–19 (2023). doi:10.1016/j.actaastro.2023.\protect\penalty-\@M08.038.

(12) Mungiguerra, S., Zuppardi, G., Spanò Cuomo, L. & Savino, R. Effects of solar panels on aerodynamics of a small satellite with deployable aero-brake. *Acta Astronaut.* **151**, 456–466 (2018). doi:10.1016/j.actaastro.2018.06.040.

(13) Palmer, E. B. IV. Stochastic satellite air drag with the ballistic coefficient random variable. Thesis, Air Force Institute of Technology (2021). https://scholar.afit.edu/etd/5091.

(14) Picone, J. M., Hedin, A. E., Drob, D. P. & Aikin, A. C. NRLMSISE-00 empirical model of the atmosphere: statistical comparisons and scientific issues. *J. Geophys. Res. Space Phys.* **107**, 1468–1483 (2002). doi:10.1029/2002JA009430.

(15) Ibrahim, S. A. & Yamaguchi, E. Comparison of solar radiation torque and power generation of deployable solar panel configurations on nanosatellites. *Aerospace* **6**, 50 (2019). doi:10.3390/aerospace6050050.

(16) NASA. *Handbook for Limiting Orbital Debris*. NASA-HDBK-8719.14 (NASA, 2008). https://standards.nasa.gov/standard/nasa/nasa-hdbk-871914.